ACS APPLIED MATERIALS & INTERFACES

Research Article

www.acsami.org

Facile Fabrication of a Silver Dendrite-Integrated Chip for Surface-Enhanced Raman Scattering

Hai-Xin Gu,[†,‡] Lin Xue,[‡] Yong-Feng Zhang,[‡] Da-Wei Li,[†] and Yi-Tao Long*[,†]

[†]Key Laboratory for Advanced Materials and Department of Chemistry, East China University of Science and Technology, Shanghai 200237, P. R. China

[‡]Shanghai Fire Research Institute of Ministry of Public Security, Shanghai 200438, P. R. China

Supporting Information

ABSTRACT: A facile approach to fabricating a surface-enhanced Raman scattering (SERS)-active chip by integrating silver dendrites with copper substrate through a one-step process was explored. The structures of dendrites were synthesized and controlled by an $AgNO_3$/PVP aqueous system, and the fabrication parameters amount of $AgNO_3$/PVP and reaction time were systematically investigated. The optimized silver dendrites, closely aggregated on the surface of the copper chip, exhibited high SERS activity for detecting rhodamine 6G at a concentration as low as 3.2×10^{-11} M. Meanwhile, the prepared SERS-active chip displayed a high thermal stability and good reproducibility. Moreover, the potential application for analysis of polycyclic aromatic hydrocarbons was demonstrated by detection of fluoranthene at a low concentration of 4.5×10^{-10} M. This SERS-active chip prepared by the convenient and high-yield method would be a promising means for rapid detection under field conditions.

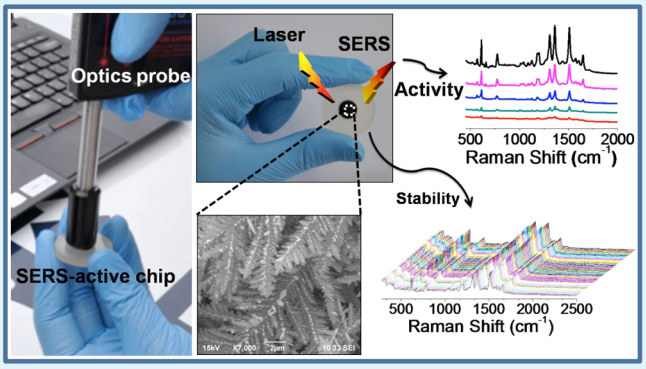

KEYWORDS: *SERS, silver dendrites, detection chip, copper substrate*

1. INTRODUCTION

Noble metal (Au, Ag, and Cu) nanomaterials possess excellent optical properties, enhancing the Raman signals of molecules when the molecules closely approach the metal surface coupled with irradiation. On the basis of the property from the interaction between nanostructured metals and molecules, surface-enhanced Raman scattering (SERS) not only provides information about vibrational fingerprints of the molecular structure but also generates ultrasensitive detection ability at the trace or even single-molecule level.[1,2] Accordingly, SERS as a powerful and versatile analytical means has attracted an increasing level of interest in the field of public security,[3] forensic analysis,[4] environmental monitoring,[5] and food safety.[6]

It is well-known that SERS activity depends on the morphologies and structures of noble metals in the nano dimension.[7−9] Therefore, the preparation of SERS-active substrates is a prerequisite for realizing high-performance SERS enhancement as well as expanding its application. Much effort has been devoted to preparing nanoparticles, including different shapes[8,10] and hierarchical structures.[11,12] Recently, hybrid nanocomposites with noble metals have been developed to generate the coupled SERS enhancement and provide a low level of interference on SERS signal background compared to organic or silica substrate.[13−17] For SERS analysis, the prepared nanoparticles need to be mixed with samples on a flat substrate or in a liquid cell prior to Raman measurements. However, the colloidal substrates created by wet-chemical methods are naturally unstable because of the uncontrollable aggregation of nanoparticles, and the precipitation of particles in solution may lead to the loss of the SERS activities of the colloids. Hence, as an ideal choice for such a problem, fabricating metal nanoparticles on a solid matrix as a detection device not only intrinsically provides more reproducible and stable SERS measurements but also facilitates the migration of SERS detection from the laboratory to in-field applications.

Silver dendrites, the special structure of silver metal, have been proven to be a high-performance SERS substrate.[18−21] However, these preparation methods were complicated or time-consuming. For example, the electrochemical equipment was always used for the deposition of silver dendrites onto an aluminum substrate[18] or to initiate the deposition of metals onto the Si substrate in the presence of a strong acid HF solution.[20] The dispersed silver dendrites could be directly prepared by reducing $AgNO_3$ with NH_2OH in an aqueous solution.[21] Unfortunately, the dendrites precipitated in the solution may be unstable and inconvenient for the on-site condition compared to the dendrites immobilized on the solid flat, hindering its further potential and extended use. Moreover, these reported works involved little attempt to develop the SERS substrates into a small detection device.

Received: December 1, 2014
Accepted: January 8, 2015
Published: January 8, 2015

DOI: 10.1021/am508403k
ACS Appl. Mater. Interfaces 2015, 7, 2931−2936

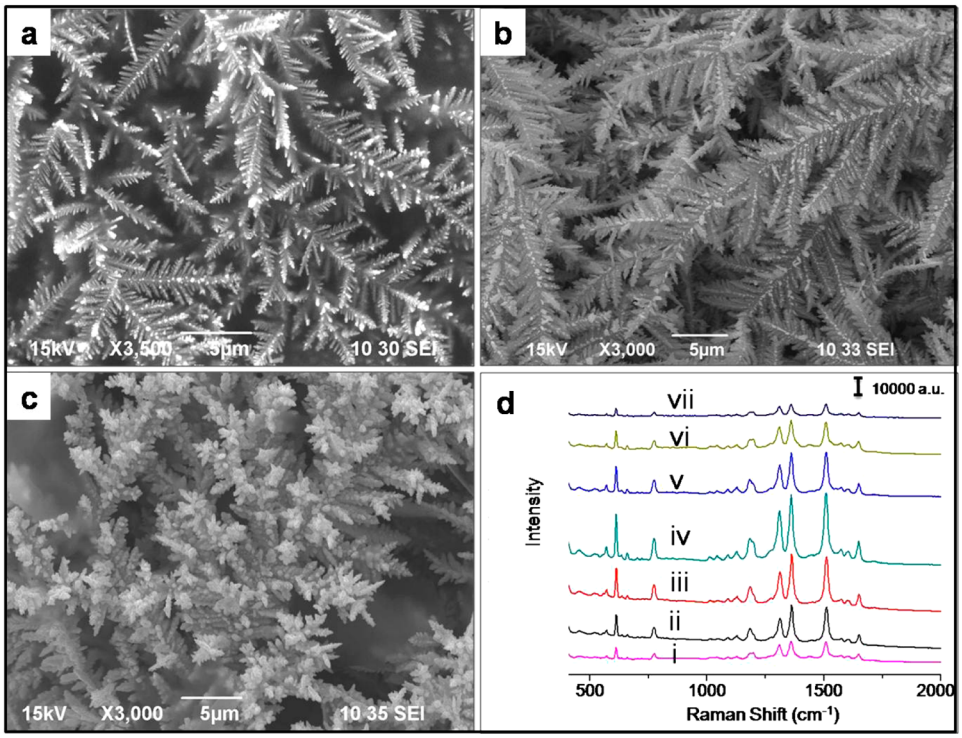

Figure 1. (a–c) SEM images of silver dendrites at $AgNO_3$:PVP ratios of 1:1, 1:5, and 1:10, respectively. (d) SERS spectra of 10^{-6} M R6G acquired on silver dendrites under designed reaction conditions at different $AgNO_3$:PVP ratios of 1:1 (curve i), 1:2 (curve ii), 1:4 (curve iii), 1:5 (curve iv), 1:6 (curve v), 1:8 (curve vi), and 1:10 (curve vii).

In this study, we present a facile and novel approach for the fabrication of silver dendrites onto a copper substrate as the detection chip by an $AgNO_3$/PVP system with no need for experimental facilities. In particular, we used $AgNO_3$ to provide the material source and growth force for silver dendrites. Meanwhile, we chose PVP to control the growth direction of the facet of the silver crystal, thus constructing the dendritic structure to optimize SERS activity. The influence of the amount of $AgNO_3$/PVP and the reaction time was systematically investigated by examining fabricated dendrites with rhodamine 6G (R6G). Three crucial parameters, SERS activity, thermal stability, and reproducibility, were investigated to verify the feasibility of the process in practical applications. To show the potential application, especially for the compounds with a low affinity for the silver surface, we further attempted to self-assemble silver dendrites with a hydrophobic alkyl chain for the detection of polycyclic aromatic hydrocarbons (PAHs). This fabricated chip would demonstrate powerful potential in practical detection under field conditions with a portable Raman spectrometer.

2. EXPERIMENTAL SECTION

2.1. Chemicals and Apparatus. All the chemicals were used without further purification. Silver nitrate (99%) and ethanol were purchased from Sigma-Aldrich (St. Louis, MO). Copper foil and polyvinylpyrrolidone (PVP) K-30 were purchased from sino-chem Co., Ltd. (Shanghai, China). R6G (99%) and 1-hexanethiol (99.9%) were obtained from Aladdin-Reagent Co., Ltd. (Shanghai, China). Ultrapure water (18 MΩ cm) was obtained from a Milli-Q System (Millipore, Billerica, MA). A portable Raman spectrometer (BWS465-785S, B&W Tek. Inc.) was used, and corresponding Raman spectra were recorded with an integration time of 3 s at an excitation wavelength of 785 nm. An ultraviolet spectrometer (Cary 500, VARIAN Inc.) equipped with the diffuse reflectance accessory and integrating sphere detector was used to investigate the properties of UV–vis absorption of the substrate.

2.2. Fabrication of Silver Dendrites on a Copper Substrate. Silver dendrites were fabricated by the reduction of silver nitrate with copper in a one-step treatment. Copper round chips ~1 cm in diameter were embedded into epoxy resin matrices (~3 cm in diameter) and mechanically polished to achieve a smooth surface. After that, the copper was rinsed with ethanol and ultrapure water in turn. Then, the copper chip was dried and immersed in the aqueous solution containing $AgNO_3$ and PVP K-30 at different ratios (1:1, 1:2, 1:4, 1:5, 1:6, 1:8, and 1:10) for a certain period of time. The treated copper chips were rinsed with water and ethanol in turn prior to vacuum drying. To modify a hydrophobic functional group onto silver dendrites, the product was placed in a 0.5 mM 1-hexanethiol/ethanol solution for 12 h at room temperature. The modified substrate was immersed in an ethanol solution to remove excess hexanethiol. Then, the obtained product was died and stored under vacuum. The sample solution with different concentrations was dropped onto the prepared substrate under ambient conditions, and the consequent analysis was recorded with a Raman spectrometer.

3. RESULTS AND DISCUSSION

3.1. Fabrication and Characterization of Silver Dendrites. In this work, we shaped the silver nanostructure through combined usage of $AgNO_3$ and PVP to achieve SERS performance. When the copper was immersed in the $AgNO_3$/PVP aqueous solution, Ag^+ acquired electrons from the Cu to form Ag metal deposited on the substrate surface. In this process, silver nanostructure forms in the process of diffusion-controlled crystal growth, and the metal morphology is subjected to silver ion concentration.[22] PVP employed as a functional capping ligand controls the growth orientation and rates of the facets of silver crystals.[10,20] It could be observed that the color of copper gradually changes to gray as the simple galvanic exchange reaction proceeds. The typical scanning

DOI: 10.1021/am508403k
ACS Appl. Mater. Interfaces 2015, 7, 2931–2936

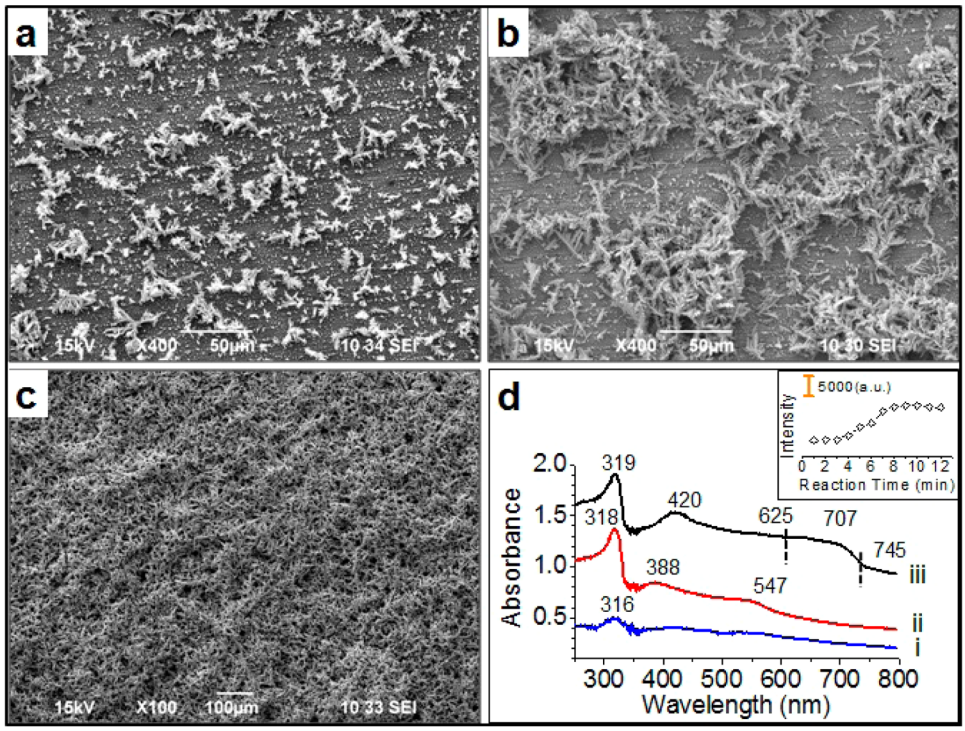

Figure 2. (a–c) SEM images of silver dendrites obtained in a $AgNO_3$/PVP (1:5) solution at 1, 5, and 9 min, respectively. (d) UV–vis absorption spectra of a silver dendrite-functionalized chip fabricated in a $AgNO_3$/PVP solution with a reaction time of 20 s (curve i), 1 min (curve ii), and 9 min (curve iii). The inset shows a plot of signal intensity of R6G vs reaction time for the band at 1360 cm^{-1}.

electron microscope (SEM) images of silver dendrites on copper surfaces prepared at different ratios of $AgNO_3$ and PVP are shown in Figure 1. It could be observed that the presence of PVP and $AgNO_3$ influenced the formation of silver dendrites. Thin-sheet dendrites were formed when the PVP:$AgNO_3$ ratio was 1:1, as shown in Figure 1a. With the increasing amount of PVP, the dendrites became sharp and thick, as shown in panels b and c of Figure 1. It indicates the growth rate and orientation of the growth of silver crystal facets were controlled in the $AgNO_3$/PVP system. To optimize the SERS performance of the substrates, R6G as a well-studied probe molecule was tested to investigate the SERS activities under different experimental conditions. Figure 1d shows the relationship between SERS detection ability and surface morphology. SERS signals intensified with the increased $AgNO_3$:PVP ratio up to 1:5 and then inversely decreased with a continuously increasing PVP concentration. Neither a deficient nor an excessive amount of PVP would improve SERS activities.

Figure 2 shows the growth of Ag dendrites in a $AgNO_3$/PVP solution with an increasing reduction time. It can be clearly observed that the dendrites grew and scattered on the copper surface (Figure 2a) at first. Then, the dendrites extended vertically and laterally (Figure 2b) to form a dense "silver jungle" coating on the whole surface of the copper substrate (Figure 2c). During this fabrication process, distinct changes in the UV–vis absorption spectra of the chip could be observed, as shown in Figure 2d. During the initial stage of the reaction (~20 s), the first band at 316 nm was observed, which results from the quadrupole resonance of the silver nanoparticles (Ag NPs).[23] With the advanced reaction time, this band slightly red-shifted to 318 nm. Meanwhile, with formation of silver dendritic structure, two new bands at 388 and 547 nm appeared, because of surface plasmon resonance and collective particle surface plasmon oscillation of silver dendrites.[24,25] Because silver dendrites grew from the copper substrate, copper as the SERS-active material may also contribute to the UV–vis absorption at 547 nm.[26] With the growth of silver dendrites, the positions of absorption bands changed further. In particular, the bands at 388 and 547 nm became broader and stronger and red-shifted to 420 and 707 nm, respectively (ranging from 625 to 745 nm), in the end with a reaction time of 9 min. Considering the edge of the absorption band located at 745 nm, an excitation wavelength of 785 nm could exhibit a good cooperative effect. Meanwhile, with the red-shift of the UV–vis absorption band and as the amount of Ag NPs increased, the spectrum signals of R6G increased and reached a high point at a time of 9 min, as shown in the inset of Figure 2d. The excess amount of silver dendrites could not help to improve the detection ability because the spot range and depth of irradiation light on the substrates are limited.

3.2. SERS Activity, Thermal Stability, and Reproducibility of the Fabricated Chip. Figure 3 shows the typical detection chip before (Figure 3a) and after (Figure 3b) fabrication under optimized conditions. Figure 3c illustrates that the sharp and dense dendrites were overlapped and constructed by closely packed Ag NPs. By determining the SERS activity with R6G, we acquired the SERS spectra of R6G at different concentrations from the prepared chips, and the detection for R6G at a concentration as low as 3.2×10^{-11} M could be achieved, as shown in Figure 4. The intensities of representative bands at 1360 cm^{-1} were plotted against the log of the concentrations (see the inset of Figure 4). The prepared structure not only generates abundant "hot spots" from the gaps formed by junctions or gaps between closely spaced particles but also provides a large surface of numerous nanoparticals for the spatial loading molecules, contributing to a significant SERS effect.

DOI: 10.1021/am508403k
ACS Appl. Mater. Interfaces 2015, 7, 2931–2936

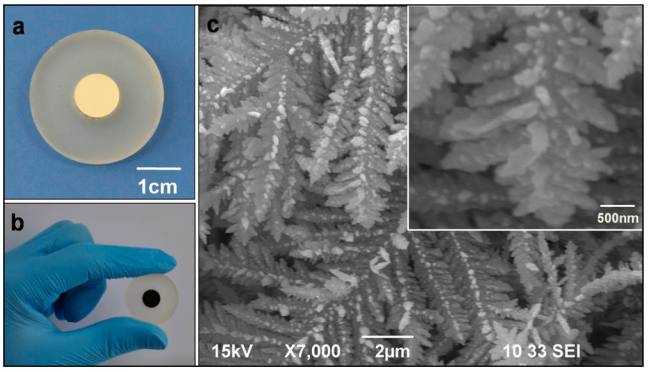

Figure 3. (a and b) Photographs of the SERS chips before and after optimized fabrication, respectively. (c) SEM image and a close-up (inset) under optimized conditions.

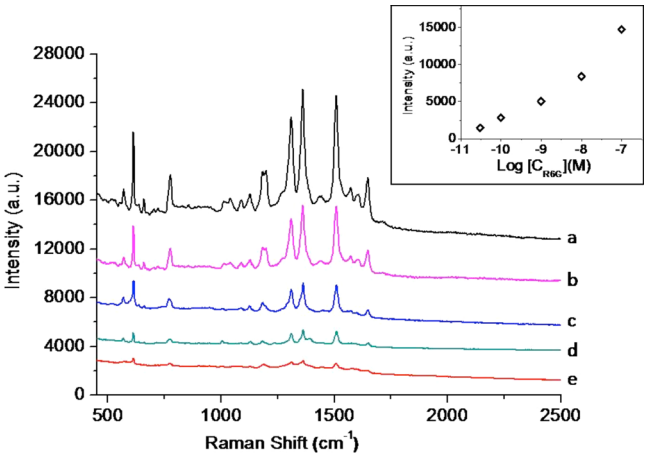

Figure 4. SERS spectra of R6G at different concentrations of (a) 1×10^{-7}, (b) 1×10^{-8}, (c) 1×10^{-9}, (d) 1×10^{-10}, and (e) 3.2×10^{-11} M acquired from SERS chips. The inset shows a plot of signal intensity vs logarithmic R6G concentration for the band at 1360 cm^{-1}.

In terms of the practical application of Raman scattering analysis, an important parameter responsible for the good performance of the SERS substrate is thermal stability. The thermal effect resulting from laser power may damage the prepared nanostructure of metals or decompose the sample molecule on the metal surface, thus weakening the SERS performance. We took intense SERS measurements to determine the stability of the SERS substrate by continuous Raman laser irradiation. Figure 5 demonstrates the stable Raman spectra acquired 50 times at the same position. This process produced a slight increase in the intensity of the Raman signals at the initial stage because of the concentration of the sample in the detection area by solution evaporation. The good thermal stability could be attributed to the high thermal conductivity of silver and copper. The substrates with a closely integrated structure could effectively transfer and reduce heat on the laser spot to limit the increase in temperature, preventing the negative thermal effect of the SERS measurement.

Apart from activity and thermal stability, the reproducibility is another important concern with respect to SERS measurement. To realize good reproducibility, before the fabrication of silver dendrites, we mechanically smoothed the surface of copper to eliminate the influence of surface irregularities. To test the reproducibility of SERS measurements, the SERS-active

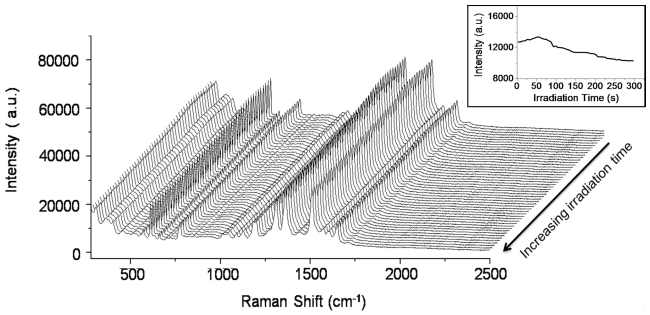

Figure 5. SERS spectra of R6G on prepared SERS chips under continuous laser irradiation (50 times) under ambient conditions, with an integration time of 3 s for each Raman spectrum and an interval time of 5 s between two SERS spectra. The inset shows the signal intensity of R6G at the 1360 cm^{-1} band vs irradiation time.

chip was immersed in a 1 μM R6G solution to immobilize molecules uniformly, and the SERS spectra were recorded from 20 random positions on a single SERS chip to investigate whether the intensity of signals on silver dendrites differs greatly from position to position, as shown in Figure 6a. The corresponding relative intensity variations at the characteristic Raman shift of 1360 cm^{-1} are listed in Figure 6b. Compared with those of recent reports,[27,28] the results indicate a good reproducibility of 15 records within ±10% (green bar), four records within ±10−20% (yellow bar), and one record slightly over 20%. This is due to the hierarchically overlapped and intercrossed dendrites (Figure 2c) improving the uniformity of the spatial structure and providing a homogeneous amount of Ag NPs within the area of the laser spot. In view of the simplicity of fabrication, low cost, and practicability, our results should be meaningful.

3.3. Detection of PAHs Using a SERS-Active Chip. The SERS effect, induced by the coupled interaction with the electric field of surface plasmon and incoming scattering light, is generated from special physical nanostructure.[9] The nanostructured dendrite was examined for its potential as a multifunctional SERS substrate. We tried to extend the substrate to widespread application even for the detection of molecules with a low affinity for a noble metal surface. PAHs, derived from the combustion process of fossil oil, are of great concern for forensic purposes in terms of ignitable liquid in arson cases. However, because of the lack of special group bonds to the metal surface, these conjoined aromatic ring compounds hardly access the region of localized surface plasmon resonance (LSPR) and thus show a poor SERS response. Therefore, the modification of a hydrophobic functional group is a necessity for capturing and enriching the PAHs from solution.[29−34] Herein, we self-assembled *n*-hexanethiol via its -SH group bonded to fabricated dendrites for the detection of fluoranthene, which is a typical PAH compound. Figure S1 of the Supporting Information shows the Raman spectra of fluoranthene obtained on silver dendrites before and after the modification of the alkyl group. It indicates the alkyl group could trap fluoranthene molecules close to the metal surface, thus yielding effective SERS measurements. Figure 7 demonstrates the ultrasensitive molecular sensing for fluoranthene at a concentration as low as 4.5×10^{-10} M. The spectral intensity increased significantly in response to an increasing analyte concentration. The SERS spectrum of fluoranthene marked with the main Raman bands is also shown in Figure 7. Briefly, Raman peaks at 556 and 665 cm^{-1}

DOI: 10.1021/am508403k
ACS Appl. Mater. Interfaces 2015, 7, 2931−2936

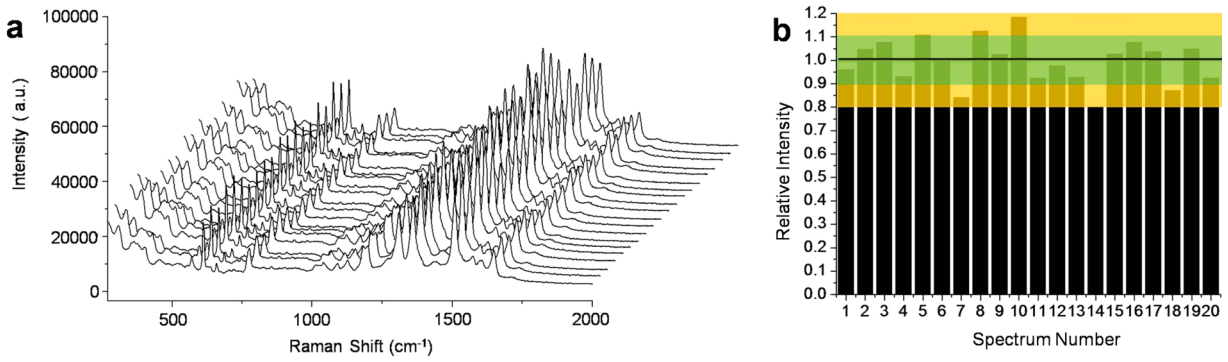

Figure 6. (a) Reproducibility of the prepared SERS substrates. SERS spectra were randomly recorded at 20 positions. (b) Intensity distribution of the 1360 cm^{-1} peak of the 20 spectra. The green and yellow zones represent ±10 and ±10−20% intensity variation, respectively.

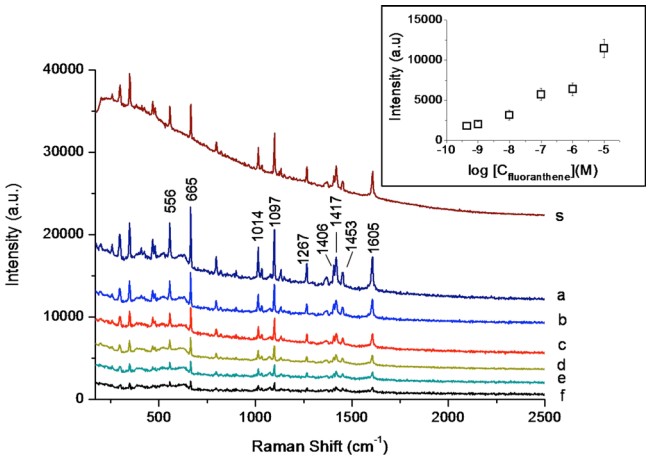

Figure 7. SERS spectra of fluoranthene at different concentrations of (a) 1×10^{-5}, (b) 1×10^{-6}, (c) 1×10^{-7}, (d) 1×10^{-8}, (e) 1×10^{-9}, and (f) 4.5×10^{-10} M obtained on *n*-hexanethiol-modified dendrites. Curve s was acquired from solid fluoranthene. The inset shows a plot of signal intensity vs logarithmic fluoranthene concentration for the band at 665 cm^{-1}.

belong to the vibration of skeletal stretching. The bands present at 1097 and 1605 cm^{-1} are assigned to vibration of C−C stretching, and the band at 1406 cm^{-1} resulted from aromatic ring vibration. The bands at 1014, 1267, 1417, and 1453 cm^{-1} are responses to C−C stretching and C−H stretching vibration.[5,35] For comparison, the Raman spectrum of solid fluoranthene (curve s) is also shown in Figure 7. The peaks of SERS spectra were quite consistent with those of the spectra of the solid state, and the peak shifts in SERS spectra were hardly observed. This is due to the weak interaction between the molecule and metal surface.[31] The fluoranthene molecules could not directly adsorp to the surface of silver dendrites because of its lack of special groups like -NH_2 and -SH, weakening the influence of the electric field of the metal surface on molecular structure. The assembled alkyl chain could trap the fluoranthene molecules close to the metal surface; however, the alkyl chain between the substrate and analytes would hinder the effective charge transfer. Thus, changes in the positions of the Raman shift and relative intensities of peaks could hardly be observed. Moreover, the SERS substrate produced little interference background.

4. CONCLUSION

A silver dendrite-integrated copper chip as a field-used SERS substrate was fabricated by a facile one-step method. The optimal fabrication conditions were determined by investigating the amount of $AgNO_3$/PVP adjustment and reaction time, and R6G was detected at a low concentration of 3.2×10^{-11} M. The prepared substrates exhibited excellent thermal stability and good reproducibility. Moreover, the nanostructured dendrite, modified by alkyl hydrosulfide with a simple self-assembly step, could achieve a high SERS sensitivity to fluoranthene. Thus, this substrate is expected to be a promising candidate for SERS detection and provide attractive potential for more widespread application.

■ ASSOCIATED CONTENT

Ⓢ Supporting Information

Raman spectra of fluoranthene acquired on the silver dendrites before and after modification of the alkyl group. This material is available free of charge via the Internet at http://pubs.acs.org.

■ AUTHOR INFORMATION

Corresponding Author

*E-mail: ytlong@ecust.edu.cn. Fax and telephone: +86-21-64250032.

Notes

The authors declare no competing financial interest.

■ ACKNOWLEDGMENTS

This research was supported by the Shanghai Municipal Natural Science Foundation (14ZR1409400, 14ZR1410800), the National Science Fund for Distinguished Young Scholars (21125522), a Shanghai Pujiang Program Grant of China (12JC1403500), and Fundamental Research Funds for the Central Universities (WB1113005).

■ REFERENCES

(1) Nie, S.; Emory, S. R. Probing Single Molecules and Single Nanoparticles by Surface-Enhanced Raman Scattering. *Science* **1997**, *275*, 1102−1106.

(2) Li, J. F.; Huang, Y. F.; Ding, Y.; Yang, Z. L.; Li, S. B.; Zhou, X. S.; Fan, F. R.; Zhang, W.; Zou, Z. Y.; Wu, D. Y.; Ren, B.; Wang, Z. L.; Tian, Z. Q. Shell-Isolated Nanoparticle-Enhanced Raman Spectroscopy. *Nature* **2010**, *464*, 392−395.

(3) Liu, H.; Lin, D.; Sun, Y.; Yang, L.; Liu, J. Cetylpyridinium Chloride Activated Trinitrotoluene Explosive Lights Up Robust and Ultrahigh Surface-Enhanced Resonance Raman Scattering in a Silver Sol. *Chem.—Eur. J.* **2013**, *19*, 8789−8796.

DOI: 10.1021/am508403k
ACS Appl. Mater. Interfaces 2015, 7, 2931−2936

(4) Raza, A.; Saha, B. Silver Nanoparticles Doped Agarose Disk: Highly Sensitive Surface-Enhanced Raman Scattering Substrate for in Situ Analysis of Ink Dyes. *Forensic Sci. Int.* **2013**, *233*, 21−27.
(5) Qu, L. L.; Li, Y. T.; Li, D. W.; Xue, J. Q.; Fossey, J. S.; Long, Y. T. Humic Acids-Based One-Step Fabrication of SERS Substrates for Detection of Polycyclic Aromatic Hydrocarbons. *Analyst* **2013**, *138*, 1523−1528.
(6) Vongsvivut, J.; Robertsona, E. G.; McNaughton, D. Surface-Enhanced Raman Spectroscopic Analysis of Fonofos Pesticide Adsorbed on Silver and Gold Nanoparticles. *J. Raman Spectrosc.* **2010**, *41*, 1137−1148.
(7) Emory, S. R.; Haskins, W. E.; Nie, S. Direct Observation of Size-Dependent Optical Enhancement in Single Metal Nanoparticles. *J. Am. Chem. Soc.* **1998**, *120*, 8009−8010.
(8) McLellan, J. M.; Li, Z.; Siekkinen, A. R.; Xia, Y. The SERS Activity of a Supported Ag Nanocube Strongly Depends on Its Orientation Relative to Laser Polarization. *Nano Lett.* **2007**, *7*, 1013−1017.
(9) Le Ru, E. C.; Etchegoin, P. G. *Principles of Surface-Enhanced Raman Spectroscopy*, 1st ed.; Elsevier: Amsterdam, 2009.
(10) Zhang, J. H.; Liu, H. Y.; Zhan, P.; Wang, Z. L.; Ming, N. B. Controlling the Growth and Assembly of Silver Nanoprisms. *Adv. Funct. Mater.* **2007**, *17*, 1558−1566.
(11) Piao, L.; Park, S.; Lee, H. B.; Kim, K.; Kim, J.; Chung, T. D. Single Gold Microshell Tailored to Sensitive Surface Enhanced Raman Scattering Probe. *Anal. Chem.* **2010**, *82*, 447−451.
(12) Chen, C.; Wong, C. Shape-Diversified Silver Nanostructures Uniformly Covered on Aluminium Micro-Powders as Effective SERS Substrates. *Nanoscale* **2014**, *6*, 811−816.
(13) Liu, Z.; Yang, Z.; Peng, B.; Cao, C.; Zhang, C.; You, H.; Xiong, Q.; Li, Z.; Fang, J. Highly Sensitive, Uniform, and Reproducible Surface-Enhanced Raman Spectroscopy from Hollow Au-Ag Alloy Nanourchins. *Adv. Mater.* **2014**, *26*, 2431−2439.
(14) Yang, Y.; Liu, J.; Fu, Z.-W.; Qin, D. Galvanic Replacement-Free Deposition of Au on Ag for Core−Shell Nanocubes with Enhanced Chemical Stability and SERS Activity. *J. Am. Chem. Soc.* **2014**, *136*, 8153−8156.
(15) Kong, C.; Lv, J.; Sun, S.; Song, X.; Yang, Z. Copper-Templated Synthesis of Gold Microcages for Sensitive Surface-Enhanced Raman Scattering Activity. *RSC Adv.* **2014**, *4*, 27074−27077.
(16) Wang, Y.; Salehi, M.; Schütz, M.; Schlücker, S. Femtogram Detection of Cytokines in a Direct Dot-Blot Assay Using SERS Microspectroscopy and Hydrophilically Stabilized Au−Ag Nanoshells. *Chem. Commun.* **2014**, *50*, 2711−2714.
(17) Pal, J.; Ganguly, M.; Dutta, S.; Mondal, C.; Negishi, Y.; Pal, T. Hierarchical Au−CuO Nanocomposite from Redox Transformation Reaction for Surface Enhanced Raman Scattering and Clock Reaction. *CrystEngComm* **2014**, *16*, 883−893.
(18) Jiang, C.; Fang, Y. Simple Method for Electrochemical Preparation of Silver Dendrites Used as Active and Stable SERS Substrate. *J. Colloid Interface Sci.* **2007**, *314*, 46−51.
(19) Gutés, A.; Carraro, C.; Maboudian, R. Silver Dendrites from Galvanic Displacement on Commercial Aluminum Foil as an Effective SERS Substrate. *J. Am. Chem. Soc.* **2010**, *132*, 1476−1477.
(20) Yan, M.; Xiang, Y.; Liu, L.; Chai, L.; Li, X.; Feng, T. Silver Nanocrystals with Special Shapes: Controlled Synthesis and Their Surface-Enhanced Raman Scattering Properties. *RSC Adv.* **2014**, *4*, 98−104.
(21) Wang, L.; Li, H.; Tian, J.; Sun, X. Monodisperse, Micrometer-scale, Highly Crystalline, Nanotextured Ag Dendrites: Rapid, Large-scale, Wet-Chemical Synthesis and Their Application as SERS Substrates. *ACS Appl. Mater. Interfaces* **2010**, *2*, 2987−2991.
(22) Fang, J.; Ding, B.; Song, X. Self-Assembly Ability of Building Units in Mesocrystal, Structural, and Morphological Transitions in Ag Nanostructures Growth. *Cryst. Growth Des.* **2008**, *8*, 3616−3622.
(23) Kelly, K. L.; Coronado, E.; Zhao, L. L.; Schatz, G. C. The Optical Properties of Metal Nanoparticles: The Influence of Size, Shape, and Dielectric Environment. *J. Phys. Chem. B* **2003**, *107*, 668−677.
(24) Zhou, Q.; Li, X.; Fan, Q.; Zhang, X.; Zheng, J. Charge Transfer between Metal Nanoparticles Interconnected with a Functionalized Molecule Probed by Surface-Enhanced Raman Spectroscopy. *Angew. Chem., Int. Ed.* **2006**, *45*, 3970−3973.
(25) Zhu, S.; Fan, C.; Wang, J.; He, J.; Liang, E. Self-Assembled Ag Nanoparticles for Surface Enhanced Raman Scattering. *Opt. Rev.* **2013**, *20*, 361−366.
(26) Lee, J. P.; Chen, D.; Li, X.; Yoo, S.; Bottomley, L. A.; EI-Sayed, M. A.; Park, S.; Liu, M. Well-Organized Raspberry-Like Ag@Cu Bimetal Nanoparticles for Highly Reliable and Reproducible Surface-Enhanced Raman Scattering. *Nanoscale* **2013**, *5*, 11620−11624.
(27) Wang, W.; Guo, Q.; Xu, M.; Yuan, Y.; Gu, R.; Yao, J. On-Line Surface Enhanced Raman Spectroscopic Detection in a Recyclable Au@SiO_2 Modified Glass Capillary. *J. Raman Spectrosc.* **2014**, *45*, 736−744.
(28) Polavarapu, L.; Porta, A. L.; Novikov, S. M.; Coronado-Puchau, M.; Liz-Marzán, L. M. SERS: Pen-on-Paper Approach Toward the Design of Universal Surface Enhanced Raman Scattering Substrates. *Small* **2014**, *10*, 3064−3070.
(29) Olson, L. G.; Uibel, R. H.; Harris, J. M. C18-modified Metal-colloid Substrates for Surface-Enhanced Raman Detection of Trace-Level Polycyclic Aromatic Hydrocarbons in Aqueous Solution. *Appl. Spectrosc.* **2004**, *58*, 1394−1400.
(30) Jones, C. L.; Bantz, K. C.; Haynes, C. L. Partition Layer-modified Substrates for Reversible Surface-Enhanced Raman Scattering Detection of Polycyclic Aromatic Hydrocarbons. *Anal. Bioanal. Chem.* **2009**, *394*, 303−311.
(31) Costa, J. C. S.; Sant'Ana, A. C.; Corio, P.; Temperini, M. L. A. Chemical Analysis of Polycyclic Aromatic Hydrocarbons by Surface-Enhanced Raman Spectroscopy. *Talanta* **2006**, *70*, 1011−1016.
(32) Leyton, P.; Córdova, I.; Lizama-Vergara, P. A.; Gómez-Jeria, J. S.; Aliaga, A. E.; Campos-Vallette, M. M.; Clavijo, E.; García-Ramos, J. V.; Sanchez-Cortes, S. Humic Acids as Molecular Assemblers in the Surface-Enhanced Raman Scattering Detection of Polycyclic Aromatic Hydrocarbons. *Vib. Spectrosc.* **2008**, *46*, 77−81.
(33) Xie, Y.; Wang, X.; Han, X.; Xue, X.; Ji, W.; Qi, Z.; Liu, J.; Zhao, B.; Ozaki, Y. Sensing of Polycyclic Aromatic Hydrocarbons with Cyclodextrin Inclusion Complexes on Silver Nanoparticles by Surface-Enhanced Raman Scattering. *Analyst* **2010**, *135*, 1389−1394.
(34) Guerrini, L.; Garcia-Ramos, J. V.; Domingo, C.; Sanchez-Cortes, S. Sensing Polycyclic Aromatic Hydrocarbons with Dithiocarbamate-Functionalized Ag Nanoparticles by Surface-Enhanced Raman Scattering. *Anal. Chem.* **2009**, *81*, 953−960.
(35) Maddams, W. F.; Royaud, I. A. M. The Characterization of Polycyclic Aromatic Hydrocarbons by Raman Spectroscopy. *Spectrochim. Acta, Part A* **1990**, *46*, 309−314.

DOI: 10.1021/am508403k
ACS Appl. Mater. Interfaces 2015, 7, 2931−2936